AFRL-AFOSR-VA-TR-2020-0052

Tunable chiroptical response in metamaterial-nanocrystal hybrid systems

Vivian Ferry
REGENTS OF THE UNIVERSITY OF MINNESOTA

10/04/2019
Final Report

Air Force Research Laboratory
AF Office Of Scientific Research (AFOSR)/ RTB1
Arlington, Virginia 22203
Air Force Materiel Command

Final Performance Report

AFOSR Grant FA9550-16-1-0282

Title: Tunable chiroptical response in metamaterial-nanocrystal hybrid systems

Grantee Institution: University of Minnesota

Program Manager: Dr. Gernot Pomrenke

Reporting Period: July 1, 2016 – June 30, 2019

PI: Prof. Vivian Ferry
Assistant Professor
University of Minnesota
421 Washington Ave SE
Minneapolis, MN 55455
Tel: 612-625-7522
Email: veferry@umn.edu

1. Objectives.

The overall objectives of this project are to understand and control light emission from colloidal nanocrystals coupled to chiral plasmonic metamaterials, and to understand nanoscale-light matter interactions in chiral environments. Chiral nanomaterials inherently couple together both electric and magnetic fields, and are therefore expected to be used in various photonic technologies, from ultrafast switches to topological photonics to document security. The majority of chiral metamaterials focus on resonant interactions between nanostructures of the same material (e.g. gold). In this project, we sought to create tunable and switchable chiral metamaterials, with the goal of controlling the polarization state of luminescent nanocrystals coupled to the chiral metamaterial, and was accomplished by building up understanding of each of the components: controlled chirality in nanocrystals, tunable chirality in metamaterials, nanopatterning methods for nanocrystals, and chiral metamaterials coupled to luminescent nanocrystals.

2. Accomplishments.

2a. Chiral semiconductor nanocrystals.

We synthesized and developed a new class of chiral nanocrystals comprised of achiral CdSe nanocrystals functionalized with chiral carboxylic acid ligands. We developed a different ligand exchange method that improves surface functionalization and allows a wide range of ligands to be tethered to the surface of the nanocrystal. By examining a series of related ligands, we achieved higher dissymmetry factors than previously reported for these materials.

2b. Chiral metamaterials with off-resonantly coupled components.

We designed a chiral metamaterial that incorporates both plasmonic and dielectric components, such that changing the refractive index of the dielectric component relative to the cladding material reverses the sign of the circular dichroism. This system does not require reconfiguration of the components to reverse the circular dichroism. The effect derives from controlling the relative absorption of the plasmonic components via scattering from the dielectric component.

2c. Chiral metamaterials coupled to luminescent nanocrystals.

We coupled light-emitting nanocrystals to a chiral metamaterial and studied the polarization state of the luminescence. We found that the polarization state and direction of the circularly polarized luminescence can be controlled by tuning the effective refractive index of the waveguide modes in the system, and that modulating the refractive index of the substrate could reverse the polarization state at particular directions. We also found that it is not critical for the light emitter to be spectrally matched to the resonance of the metamaterial, opening up a broader set of materials that can be integrated into these systems.

2d. Nanopatterned nanocrystals as components of light-emitting metamaterials.

We developed a nanopatterning process to transform colloidally synthesized semiconductor nanocrystals into nanopatterned solids. We used direct-write electron beam lithography to crosslink the nanocrystals, forming structures with lateral sizes below 30 nm and aspect ratios between 2 and 3, which can act as the components of light-emitting metamaterials.

3. Chiral semiconductor nanocrystals

Semiconductor nanocrystals can exhibit chiroptical properties on their own, an effect that could be amplified by integrating these materials with chiral metamaterials. These nanocrystals can be made chiral by various routes, including shape-directed synthesis that preferentially creates chiral shapes, or the attachment of chiral ligands to the surface of otherwise achiral nanoparticles. While the former often offers stronger dissymmetry effects, the latter is advantageous because high-quality nanocrystals can be synthesized separately, and these chiroptical properties can be precisely tailored by controlling the ligand-surface binding. The challenge is the low dissymmetry factors of these nanocrystals.

The dissymmetry factor is defined as $g = \frac{A_L - A_R}{A}$, where A_L is the absorption under left-handed circularly polarized illumination, and A_R is the absorption under right-handed circularly polarized light. Previous literature reports indicated that the dissymmetry factor for CdSe nanocrystals was approximately 10^{-5}. By systematically tailoring the ligand on the surface, we realized nanocrystals with dissymmetry factors as high as 7×10^{-4} (Puri and Ferry, ACS Nano, 2017). The nanocrystals are originally synthesized using non-hot injection methods and are achiral. The replacement of the original ligands with chiral ligands results in circular dichroism (CD) associated with the excitonic features of the CdSe nanocrystals. Key to our work was the

development of an alternative ligand exchange method: in the previously published work, the nanocrystals are first treated with a base to promote exchange, whereas in our method the ligand exchange proceeds directly (and in 5 minutes rather than overnight). This allowed us to investigate a larger set of ligands to evaluate the chiroptical properties.

We compared the dissymmetry factors from 10 different ligands, comparing thiol and carboxyl bonds, monocarboxylic and dicarboxylic acids, and the effects of multiple stereocenters on the optical response. This family of related ligands resulted in 30x difference in dissymmetry factors. We identified a few key trends: first, similar ligands that bind to the nanocrystal differently (thiol vs. carboxylic acid) produce circular dichroism spectra that appear to be shifted from one another, despite no changes in the size of the crystal. Second, ligands with multiple binding sites, and therefore the potential for bidentate interactions, exhibit stronger dissymmetry factors. Third, ligands with multiple stereocenters, such as tartaric acid, exhibit stronger effects than ligands with a single stereocenter. These results can be explained using a simple model where the ligand induces splitting into the excitonic structure of the CdSe nanocrystals.

For photonic applications, one of the most intriguing features is the difference in sign of the circular dichroism spectrum at particular wavelengths due to the binding of the ligand to the surface, as illustrated in Fig. 1(c) below. In this case, by changing the ligand structure slightly, there is a reversal in the sign of the CD spectrum. These structures could be made dynamic to

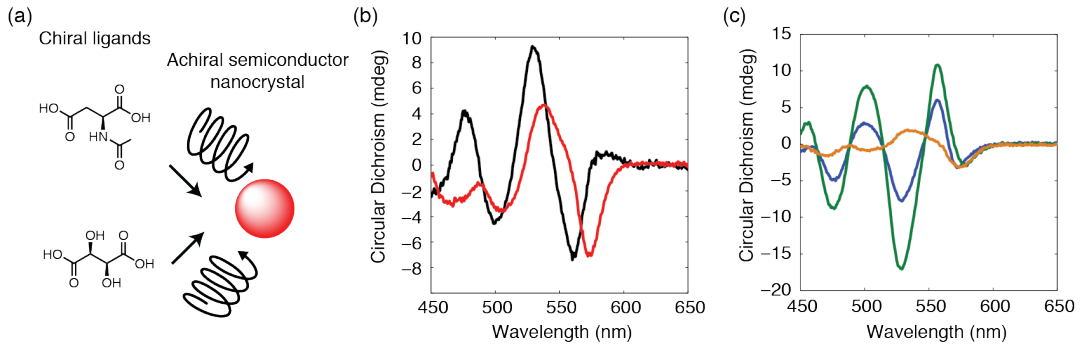

Figure 1: Chirality can be transferred into an achiral nanocrystal by attaching chiral ligand to the surface. The chirality induced into the nanoparticle by the ligand depends on the interaction strength of the ligand with the nanocrystal. Circular dichroism spectra are shown for ligands bound to 4.2 nm CdSe nanoparticles near the exciton transitions of the CdSe nanoparticles. (a) Red: N-acetyl-L-cysteine, Black: N-acetyl-L-aspartic acid. The shift in the CD spectrum is indicative of the splitting of the excitons by the ligands, with the difference due to the binding group attached to the CdSe surface. (b) Orange: L-(+)-lactic acid, Blue: D-(+)-malic acid, Green: L-(+)-tartaric acid. Increasing the number of stereocenters leads to enhanced dissymmetry factors.

create a new sensing mechanism, where tailored ligands capture an achiral analyte, changing the binding of the ligand to the nanocrystal surface, and detected through a change in circular dichroism. Similarly, such materials could be turned into tunable photonic materials by changing the configuration of the ligand.

4. Chiral metamaterials with off-resonantly coupled components.

The host-guest system is one where the structures that comprise the chiral metamaterial interact off-resonantly. This type of system offers several advantages, since tuning the properties of one material influences the collective properties of the system. We designed this system so that the sign of the circular dichroism would reverse as the refractive index of one component changes, without necessitating any reconfiguration or movement of the parts.

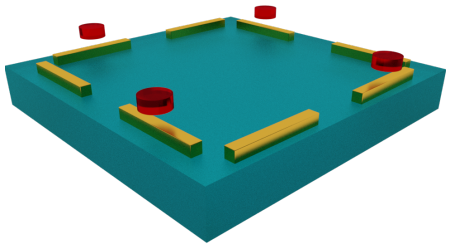

Figure 2: Schematic of off-resonant structure with a dielectric disk located in the plane above two resonantly matched nanorods.

Our system is a chiral metamaterial comprised of a mixture of plasmonic and dielectric components. The general layout is shown in Fig. 2, and consists of two resonantly coupled gold bars in a lower plane with a dielectric disk in an upper plane (Pachidis and Ferry, Optics Express, 2018). The system is chiral because of the presence of the dielectric disk. It is assumed that there is a spacer layer surrounding the rods and disk. This structure was designed so that the dielectric disk can only interact with the rods via scattering, as the disk itself does not absorb.

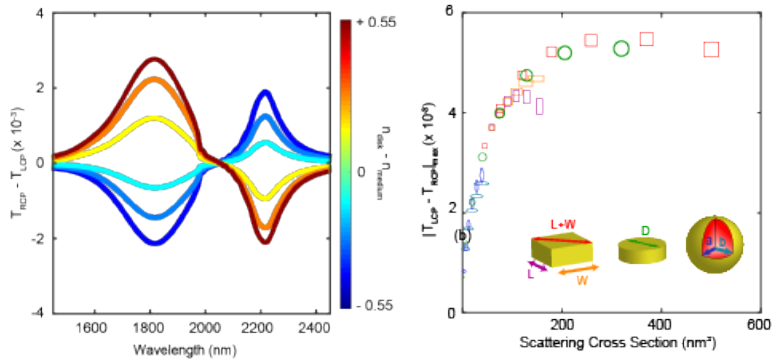

Figure 3: Simulations showing the difference in transmission under RCP and LCP illumination as the refractive index of the dielectric disk changes. The color bar is the difference in refractive index between the disk and the cladding medium. Changing the index to be greater than or less than the surrounding medium reverses the sign of the chiropotical response.

We found that as the refractive index of the disk is modified around the index of the cladding medium (Fig. 3), the polarization state that is predominantly absorbed reverses. This effect arises because the refractive index changes which nanorod absorbs more light. The nanorod located under the disk absorbs more LCP light, whereas the other nanorod absorbs more RCP light. Without the disk, the absorption between each nanorod is equal, leading to no net chirality. In the presence of the disk, the refractive index of this dielectric component either enhances or suppresses the absorption of the nanorod underneath it, resulting in unequal amounts of absorption and therefore net chiroptical properties.

Since this effect arises solely from scattering; it is important that the dielectric disk is located in the center of the nanorod to avoid detuning the resonance of one nanorod from the other. The overall magnitude of the effect does not depend on the shape of the dielectric component; instead it scales with the scattering cross section of the dielectric object, as shown in Fig. 3.

Importantly this reversibility is also mirrored in the optical chirality of the electromagnetic fields in the plane over the metamaterial. The optical chirality is given by

$$\boldsymbol{C} = -\frac{\boldsymbol{\varepsilon_0 \omega}}{\boldsymbol{2}} \boldsymbol{\Im}(\boldsymbol{B}(\boldsymbol{r}) \cdot \boldsymbol{E}(\boldsymbol{r})^*)$$

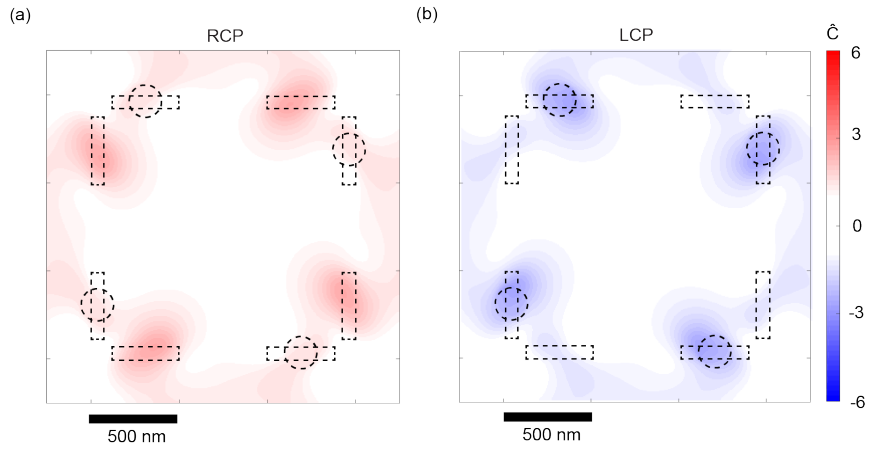

Figure 4: Calculations of the optical chirality enhancement for a system with $n_{disk} = 1$ at $\lambda = 1815$ nm (high energy CD resonance peak). A cross section is shown at 10 nm above the top side of the disks under (a) RCP and (b) LCP illumination. These calculations indicate significant enhancement in the optical chirality at a location where emitters could be placed above the metamaterial.

and the optical chirality enhancement normalizes this quantity to the optical chirality of circularly polarized light.

$$\widehat{\boldsymbol{C}} = \frac{\boldsymbol{C}}{|\boldsymbol{C}_{CPL}|}$$

Achiral light emitters coupled to regions of enhanced optical chirality are expected to exhibit circularly polarized luminescence corresponding to the sign of the optical chirality. In our system, the structure could therefore show reversibility as the refractive index changes: a layer of light emitting material cast over the top of the structure would exhibit reversible CPL without moving any of the metamaterial components (Fig. 4).

5. Chiral metamaterials coupled to luminescent nanocrystals.

Illuminating a chiral metamaterial with linearly polarized light also produces circularly polarized luminescence from nearby light emitters. In most cases, however, the pattern is fixed upon fabrication, making it difficult to tune the polarization state of the circularly polarized luminescence. We investigated coupling between light-emitting nanocrystals and a chiral metamaterial pattern, finding that by engineering the effective index of the modes in the structure, the polarization state in particular directions can be reversed (Pachidis, Cote, and Ferry, ACS Applied Nano Materials, 2019).

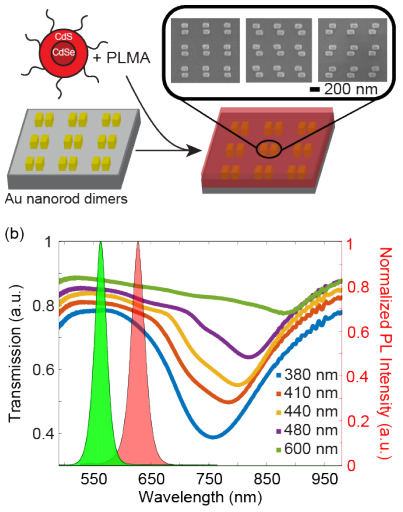

Figure 5: Overview of system, consisting of patterned Au nanorod dimers coated in a 35 nm layer thick film of light-emitting nanocrystals embedded in PLMA. (b) Unshaded spectra show the transmission of the Au nanoarray, shaded spectra show the photoluminescence from CdSe/CdS nanocrystals (red) and CdSe/ZnS nanocrystals (green).

The general structure is shown in Fig. 5, and consists of gold nanobars, either arranged parallel to one another (achiral) or offset (chiral). The pitch between the pairs of nanobars is varied, as shown in the transmission spectra. A film of light-emitting semiconductor nanocrystals embedded in a poly laurylmethacrylate matrix is coated over the top of the nanorods, with photoluminescence spectra that are deliberately detuned from the resonance of the nanobars. The luminescent layer is approximately 40 nm thick. A blue laser illuminates the sample, and using back-plane focal imaging coupled to a polarimeter, we detect the polarization

state of the photoluminescence in each direction. We measure the degree of circular polarization (DCP) of the sample by measuring the Stokes parameters of the system, such that

$$DCP = \frac{S_3}{S_0}$$

The branches seen in the Fourier plane images indicate that light is outcoupled from the structure at the directions predicted for Rayleigh-Wood anomalies, as described by the following expression

$$\left(\frac{2\pi}{\lambda_{PL}} n_{mode}\right)^2 = \left(\boldsymbol{k}_x - N_x \frac{2\pi}{pitch}\right)^2 + \left(\boldsymbol{k}_y - N_y \frac{2\pi}{pitch}\right)^2$$

where k_x and k_y are the wavevectors of the outcoupled luminescence and N_x and N_y denote the grating orders. The pitch is a square lattice, which simplifies the expression. Incident light excites the nanocrystals, which luminescence and couple into the waveguide modes of the structure. These modes interact with the pattern at grazing incidence and are outcoupled along the Rayleigh-Wood anomalies. Therefore, the modes will change if the wavelength of the photoluminescence of the emitter changes, if the pitch changes, or if the effective refractive index of the mode changes.

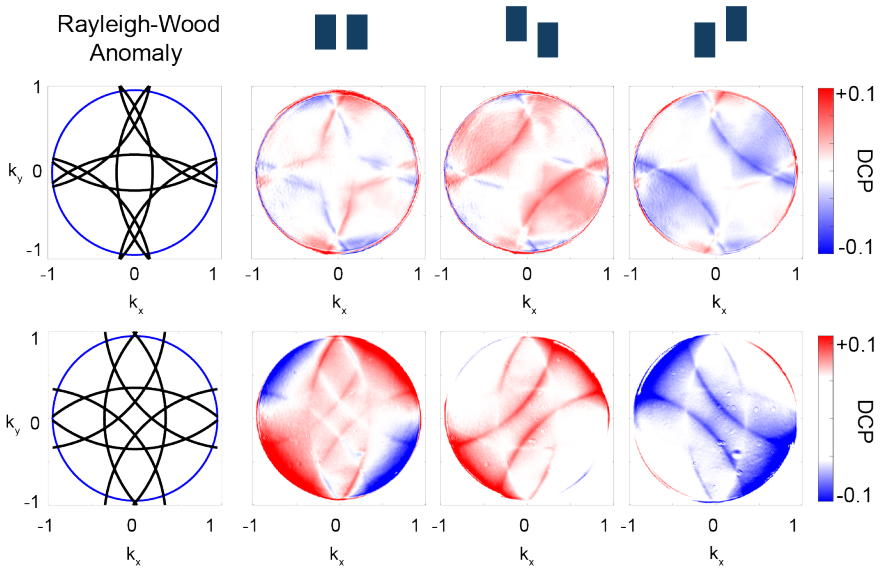

Figure 6: Degree of circular polarization data measured using k-space spectroscopy for (a) CdSe/CdS nanocrystal composite and (b) CdSe/ZnS nanocrystal composite coupled to metallic nanorod dimer arrays with pitch = 480 nm. Both show agreement between the calculated Rayleigh-Wood anomalies and the observed outcoupled modes, despite the significant mismatch between the photoluminescence maximum wavelength and the resonance of the metamaterial.

We systematically studied the role of different materials in this system. First, even when the emitter is significantly bluer than the dominant resonance of the metamaterial pattern (Fig. 6), the luminescent light still follows the directions predicted by the Rayleigh-Wood calculations. In the case of the achiral pattern, certain directions exhibit polarized luminescence due to striking the pattern at oblique incidence, but the effect cancels out when integrated over angle. For the two chiral patterns, particular directions are outcoupled preferentially, with a corresponding polarization state dominating the response. These are mirror images of one another. A similar experiment using a further detuned nanocrystal (CdSe/ZnS core/shell nanocrystals) exhibits the same dependence, with accordingly shifted directions as the wavelength of PL shifted. Changing the refractive index of the luminescent layer on top (i.e. using a neat film of nanocrystals instead of embedding into a polymer) does not affect the measured direction of polarization or the degree of circular polarization. This indicates that a mixture of different light emitters could be coupled to an individual pattern, without needing to redesign the pattern.

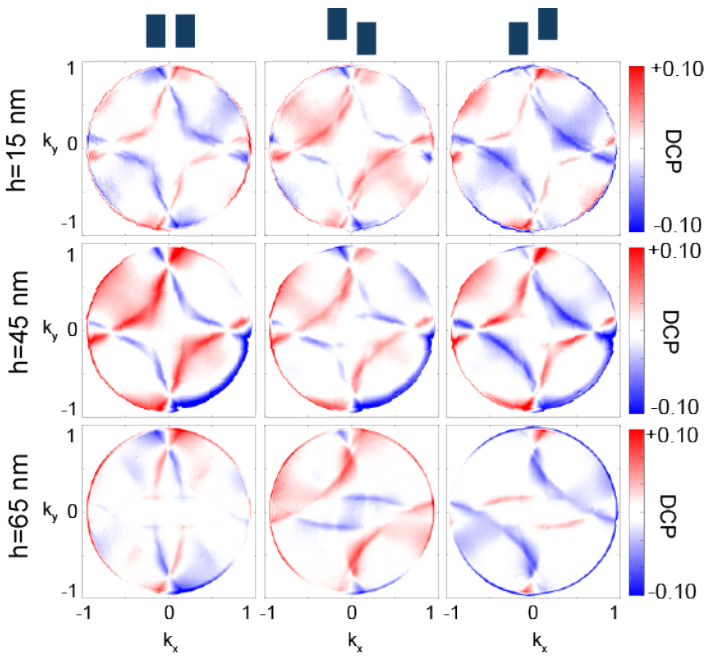

Figure 7: Degree of circular polarization of luminescent light for a system with an alumina spacer layer inserted between the gold and the luminescent material. The three rows denote different thicknesses of the alumina layer. The similar magnitude of DCP in all cases indicates that the effect arises from waveguide modes determined by the arrangement of nanostructures rather than local resonances that are confined to the near field.

The direction could be tuned actively by changing the effective index of the modes of the structure. Calculations of the effective index indicate that there is no significant change as the thickness of the luminescent layer is increased, until it reaches 315 nm thick. We found that adding a spacer layer of a similar refractive index to the QD-PLMA composite (Al_2O_3) on top of the gold doesn't significantly change the polarization directions, but is advantageous since it removes luminescence quenching of the nanocrystals by the gold (Fig. 7).

However, inserting a different refractive index substrate has a significant effect on the direction and polarization state

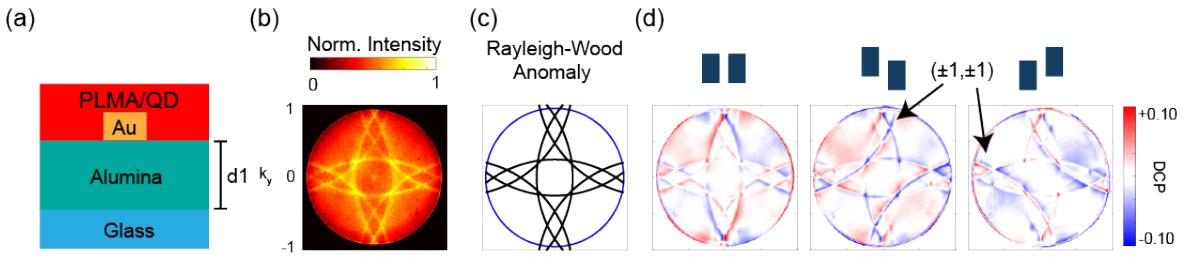

Figure 8: (a) Schematic of structure with alumina included below the Au pattern. The alumina is 294 nm thick. (b) Measured intensity of photoluminescence measured with k-space spectroscopy. (c) Calculated Rayleigh-Wood anomalies. (d) Measured degrees of circular polarization. Compared to the similar case without the alumina substrate, the (±1,0) and (0,±1) modes exhibit the same sign of circular polarization, while the (±1,±1) modes reverse sign.

measured. When a ~300 nm thick layer of Al_2O_3 is inserted between the glass substrate and the gold pattern, the effective refractive index of the mode switches to $n = 1.56$ from $n = 1.52$. In addition to shifting the directions of outcoupled light, there is a notable reversal in the polarization state along specific branches (Fig. 8). The (±1,0) and (0,±1) modes exhibit the same polarization signatures as the example on glass, whereas the (±1, ±1) modes invert. The observed pattern matches the effective refractive index of the modes with the most overlap with the luminescent layer. This indicates that changing the refractive index of a substrate, for example electrically, could be a straightforward method to tune the polarization state at specific directions.

To build on this, we fabricated the same structures on top of a thick layer of silicon nitride that supports multiple modes. Based on the measured data, the Rayleigh-Wood anomaly measurements now show evidence of three different effective index modes, which match to the calculated modes predicted to have the highest field concentration within the nanocrystal-polymer composite. This produces a complex system with multiple guided modes that are outcoupled at different angles with different polarization dependence, but can be understood in this framework of manipulating the effective index of the modes in the overall structure.

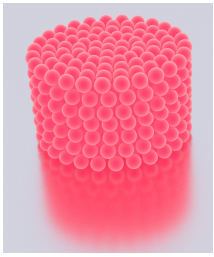

Figure 9: Schematic overview of patterned nanocrystal solid, comprised of light-emitting semiconductor nanocrystals organized into a solid with its own optical properties.

5. Nanopatterned nanocrystals as components of light-emitting metamaterials.

In the above examples, the quantum dots are deposited in a film

or embedded in a matrix over the patterns, but different tunability could be created if the nanocrystals were placed deterministically. Although there are some methods for positioning individual nanocrystals, very different systems can be studied if the nanocrystals are instead arranged into patterns, at the scale and aspect ratios that allow them to exhibit hierarchical properties that combine both the individual quantum confined effects of the nanocrystal and the resonances of the overall shape (Fig. 9). In addition to chiroptical properties, such patterns could form the basis for light-emitting metamaterials.

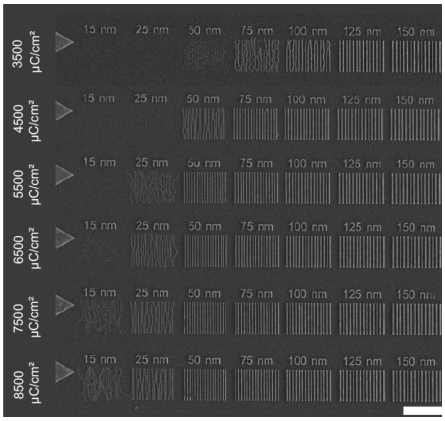

Figure 10: SEM image of patterned quantum dot solids with increasing electron beam dose. The width of the lines is indicated above each pattern. We are able to successfully pattern structures with feature sizes < 30 nm. Scale bar is 3 µm.

There are several demanding requirements for these nanoscale patterns to actually exhibit these properties. First, with refractive index values of ~1.9, the patterns should be high aspect ratio and not monolayers to exhibit their own resonances. Additionally, the method must be capable of nanoscale resolution, be robust to sonication and capable of patterning near other materials with good accuracy, and preserve photoluminescence after patterning. This latter specification makes methods that do not require modified ligands or liftoff with polar solvents advantageous. Although there are many methods for patterning nanocrystals, such as transfer printing and ink jet printing, these methods do not meet all of the above requirements.

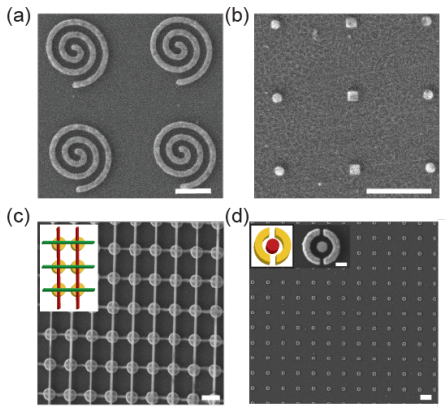

Figure 11: SEM images showing examples of patterned structures. (a) Spirals comprised of CdSe/CdS nanocrystals. Scale bar: 1 µm. (b) CdSe/CdS structures of disks and squares. Scale bar: 500 nm. (c) Multiple exposures are also possible. The bottom layer consists of Au disks, with two different deposition and patterning steps of overlapping CdSe/CdS nanocrystal lines as depicted in the inset. Scale bar: 500 nm. (d) Disk of CdSe/CdS positioned in the center of Au rings, with greater than 99% accuracy. Scale bar: 2 µm. Inset scale bar: 200 nm.

We have shown that direct-write electron beam lithography addresses all of these challenges (Dement, Quan, Ferry, ACS Applied Materials and Interfaces, 2019). In direct-write electron beam lithography, the

nanocrystals themselves are used as the resist. Upon exposure, the ligands between the particles crosslink, creating an insoluble mass in the regions of exposure. After rinsing with the original solvent, the exposed regions remain anchored to the substrate. We found that the spatial resolution of this method can be significantly improved by first functionalizing the surface with a nonspecific reagent, octadecyltrichlorosilane, which both aids in wetting the surface to create denser films and provides additional covalent bonding point to attach the nanocrystals to the surface. Increasing the dose improves the resolution, and we have been able to successfully pattern feature sizes < 30 nm.

These patterned nanocrystals additionally meet the other demands listed above. We have been able to write patterns with aspect ratios of 2 – 3. Sonication does not disrupt the patterns. Multiple electron beam exposures can be done on a single substrate. For example, we have been able to position patterned luminescent nanocrystals in the middle of split ring resonators with greater than 99% placement accuracy, and write multiple layers of nanocrystals on top of one another in separate depositions and exposures. We have written various structures including spirals and hole arrays. We can additionally pattern on both silicon and indium tin oxide substrates.

The optical properties of these structures are preserved upon patterning. While there is some initial loss in photoluminescence intensity upon exposure, the photoluminescence intensity is independent of exposure dose, and no spectral shifts are observed. Characterization of the refractive index before and after patterning indicates a very slight increase in the index after exposure, but the effect is small. This indicates that the patterning process preserves the desirable

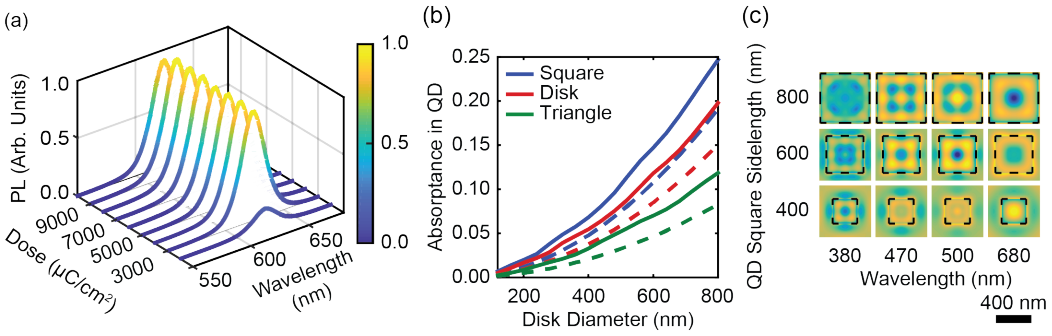

Figure 12: Optical properties of patterned solids. (a) PL as a function of electron beam dose. (b) Simulations comparing the absorption calculated in a quantum dot solid (solid line) to an equivalent volume extracted from a continuous film (dashed) for various shapes. (c) Simulations showing electric field intensity within quantum dot solid square pillars of various sizes, at selected wavelengths.

properties of the individual nanocrystals, such as the individual luminescence and individual particle properties. However, to be useful as elements of light-emitting metamaterials, these materials must also support optical resonances determined by the shape of the pattern. We conducted simulations on these patterns using the measured refractive index to study the modes that are present in these structures. We find that these patterned structures exhibit significant scattering cross sections, and exhibit enhanced absorption compared to equivalent volumes extracted from unpatterned layers, as shown in Fig. 12.

6. Personnel Supported.

Pavlos Pachidis, Chemical Engineering PhD student.
Bryan Cote, Chemical Engineering PhD student.
Dr. Mayank Puri, postdoc. Now Senior Product Development Engineer at 3M.
Dr. Dana Dement, postdoc. Now Research Scientist at AEgis Technologies.

7. Publications.

Pavlos Pachidis, Bryan M. Cote, and Vivian E. Ferry, "Chiral nanorod dimer arrays coupled to achiral luminescent quantum dot films for directional circularly polarized photoluminescence," *ACS Applied Nano Materials,* in press. https://doi.org/10.1021/acsanm.9b01198

Dana B. Dement, Matthew K. Quan, and Vivian E. Ferry, "Nanoscale patterning of colloidal nanocrystal films for nanophotonic applications using direct write electron beam lithography," *ACS Applied Materials and Interfaces,* 11, 14970 – 14979 (2019). http://dx.doi.org/10.1021/acsami.9b01159

Pavlos Pachidis and Vivian E. Ferry, "Tunable optical chirality in a metamaterial platform with off-resonantly coupled metal-dielectric components," *Optics Express,* 26, 17289 – 17298 (2018). https://dx.doi.org/10.1364/OE.26.017289

Mayank Puri and Vivian E. Ferry, "Circular dichroism of CdSe nanocrystals bound by chiral carboxylic acids," *ACS Nano,* 11, 12240 – 12246 (2017). http://dx.doi.org/10.1021/acsnano.7b05690

8. Presentations. (presenting author marked with *)

1. V. E. Ferry*, "Tunable chiral optical properties in semiconductor nanocrystals and metamaterials," Chemistry at the Space Time Limit symposium, American Chemical Society, San Diego, CA, Aug. 2019 (invited).

2. D. B. Dement*, M. K. Quan, and V. E. Ferry, "Nanoscale patterning of colloidal films using direct write electron beam lithography," IPRIME annual meeting, Minneapolis, MN, 2019 (oral and poster).

3. B. M. Cote* and V. E. Ferry, “Optically active, chiral quantum dots: etching effects and transfer to the solid-state,” IPRIME annual meeting, Minneapolis, MN, 2019 (poster).

4. P. Pachidis* and V. E. Ferry, “Chiral response of achiral fluorescent materials coupled to chiral arrays of nanorod dimers,” IPRIME annual meeting, Minneapolis, MN, 2019 (talk and poster).

5. V. E. Ferry*, “Optical nanomaterials: chirality and patterned quantum dot solids,” Montana State University, Physics Department Seminar, Bozeman, MT, Apr. 2019 (invited).

6. V. E. Ferry*, “Optical nanomaterials: chirality, refractive index, and application to solar energy conversion,” Georgia Institute of Technology, Materials Science and Engineering Department Seminar, Atlanta, GA Mar. 2019 (invited).

7. V. E. Ferry*, “Optical nanomaterials: chirality, refractive index, and application to solar energy conversion,” Northrop Grumman, Los Angeles, CA, Nov. 2018 (invited).

8. V. E. Ferry*, “Optical nanomaterials: chirality, refractive index, and application to solar energy conversion,” California Institute of Technology, Applied Physics Department Seminar, Oct. 2018 (invited).

9. V. E. Ferry*, “Optical nanomaterials: chirality, refractive index, and application to solar energy conversion,” University of Southern California, Chemical Engineering, Materials Science, and Petroleum Engineering Department Seminar, Los Angeles, CA, Oct. 2018 (invited).

10. P. Pachidis* and V. E. Ferry, “Tunable optical chirality in a metamaterial platform with off-resonantly coupled metal–dielectric components,” Gordon Research Conference on Nanophotonics, Newry, ME, 2018 (poster).

11. P. Pachidis* and V. E. Ferry, “Chiral Metamaterial Platform with Tunable Near and Far Field Chiroptical Response,” Materials Research Society Spring meeting, Phoenix, AZ, 2018 (oral).

12. M. Puri* and V. E. Ferry, “Circular dichroism of CdSe nanocrystals bound by chiral carboxylic acids,” American Chemical Society Spring meeting, New Orleans, LA, 2018 (oral).

13. P. Pachidis* and V. E. Ferry, “Switchable chiral metamaterial platform with superchiral electromagnetic hotspots,” AIChE, Minneapolis, MN, 2017 (oral).

14. M. Puri*, and V. E. Ferry, “Examining the Optical Effects of Chiral Carboxylic Acids Bound to the Surface of CdSe Nanoparticles,” AIChE, Minneapolis, MN, 2017 (oral).

15. V. E. Ferry*, Tuning chiral properties in assemblies of plasmonic nanocrystals,” Multi-metallic plasmonics, SciX, Reno, NV, October 2017 (invited).

16. V. E. Ferry*, “Controlling optical properties of semiconductor nanocrystals: chiral quantum dots and luminescent solar concentrators,” Nanoscale luminescent materials symposium, Electrochemical Society, Seattle, WA, May 2018 (invited).

9. Awards

Marion Milligan Mason Award for Women in the Chemical Sciences, AAAS, 2019
APS Ovshinsky Fellowship for Sustainable Energy, 2019
McKnight Land-Grant Professor, 2017 – 2019, University of Minnesota
Technology Review’s 35 Innovators under 35, 2016

REPORT DOCUMENTATION PAGE

Form Approved
OMB No. 0704-0188

1. REPORT DATE *(DD-MM-YYYY)*	2. REPORT TYPE	3. DATES COVERED *(From - To)*
08-06-2020	Final Performance	01 Jul 2016 to 30 Jun 2019

4. TITLE AND SUBTITLE
Tunable chiroptical response in metamaterial-nanocrystal hybrid systems

5a. CONTRACT NUMBER

5b. GRANT NUMBER
FA9550-16-1-0282

5c. PROGRAM ELEMENT NUMBER
61102F

6. AUTHOR(S)
Vivian Ferry

5d. PROJECT NUMBER

5e. TASK NUMBER

5f. WORK UNIT NUMBER

7. PERFORMING ORGANIZATION NAME(S) AND ADDRESS(ES)
REGENTS OF THE UNIVERSITY OF MINNESOTA
200 OAK ST SE 224
MINNEAPOLIS, MN 55455-2009 US

8. PERFORMING ORGANIZATION REPORT NUMBER

9. SPONSORING/MONITORING AGENCY NAME(S) AND ADDRESS(ES)
AF Office of Scientific Research
875 N. Randolph St. Room 3112
Arlington, VA 22203

10. SPONSOR/MONITOR'S ACRONYM(S)
AFRL/AFOSR RTB1

11. SPONSOR/MONITOR'S REPORT NUMBER(S)
AFRL-AFOSR-VA-TR-2020-0052

12. DISTRIBUTION/AVAILABILITY STATEMENT
A DISTRIBUTION UNLIMITED: PB Public Release

13. SUPPLEMENTARY NOTES

14. ABSTRACT

The overall goal of this project was to create tunable and/or switchable chiral materials that exhibit circularly polarized luminescence. The most significant accomplishments of this project are: 1) development of chiral CdSe nanocrystals with high dissymmetry factors; 2) design of a tunable chiral metamaterial based on refractive index; 3) circularly polarized luminescence from nanocrystals coupled to a chiral metamaterial where tuning the refractive index of the substrate switches the polarization state along specific directions; and 4) development of patterned nanocrystal solids as components of light-emitting chiral metamaterials. In the first case, we developed a ligand exchange strategy to tether chiral carboxylic acid ligands to the surface of CdSe nanocrystals, and showed that the range of available ligands leads to a 30x range in dissymmetry factors. We also found that tartaric acid ligands lead to strong dissymmetry factors of 7x10-4, showing that ligand design significantly impacts both the spectral chiroptical response and the magnitude. We then studied a chiral metamaterial composed of plasmonic Au nanorods and a dielectric nanostructure, where the dielectric structure is both essential to render the system chiral and only interacts with the Au structures via scattering. By changing the refractive index of the disk, we modify which nanorod absorbs more light, which reverses the sign of the circular dichroism. Notably this does not involve reconfiguration of the component structures, and so does not switch to the enantiomer, but could instead lead to fast switching of the response. We then created chiral metamaterials, deposited films of achiral light emitters over the top of the structures, and measured the degree of circular polarization of luminescent light along specific directions.

15. SUBJECT TERMS
chiroptical, chiral, metamaterials, nanocrystals, nanoantennas, chiral plasmonic metamaterials, polarization, quantum dots

16. SECURITY CLASSIFICATION OF:			17. LIMITATION OF ABSTRACT	18. NUMBER OF PAGES	19a. NAME OF RESPONSIBLE PERSON
a. REPORT	b. ABSTRACT	c. THIS PAGE			POMRENKE, GERNOT
Unclassified	Unclassified	Unclassified	UU		19b. TELEPHONE NUMBER *(Include area code)* 703-696-8426